SCIENTIFIC COMMUNICATIONS

FLOATING GOLD GRAINS AND NANOPHASE PARTICLES PRODUCED FROM THE BIOGEOCHEMICAL WEATHERING OF A GOLD-BEARING ORE

Jeremiah Shuster,[1,†,*] Maggy Lengke,[2] María Florencia Márquez-Zavalía,[3,4] and Gordon Southam[1]

[1] *School of Earth Sciences, University of Queensland, St. Lucia, Queensland, Australia*

[2] *Department of Earth Sciences, University of Western Ontario, London, ON, Canada*

[3] *Instituto Argentino de Nivología, Glaciología y Ciencias Ambientales (IANIGLA), CRICYT (CONICET), Av Ruiz Leal s/n, Parque Gral. San Martín, 5500, Mendoza, Argentina*

[4] *Mineralogía y Petrología, FAD, Universidad Nacional de Cuyo, Centro Universitario, 5502, Mendoza, Argentina*

Abstract

A gold-bearing ore from the San Salvador vein, Capillitas mine, Argentina, was exposed to an enriched, iron- and sulfur-oxidizing bacterial consortium for two months in an experimental system that represented an oxidized, acid-leached weathering environment. Within this laboratory model, the dissolution of metal sulfide minerals by the bacterial consortium liberated gold grains that floated on water. Surficial crevices on grains contained detrital material associated with μm-scale, gold-rich bacteriomorphic structures interpreted to be relics of gold dissolution. The presence of nanophase gold particles, i.e., colloids and octahedral platelets, was attributed to gold reprecipitation. These secondary gold structures suggest that gold dissolution/reprecipitation, i.e., cycling, was occurring concurrently with the bacterially catalyzed dissolution of metal sulfides. The flake-like morphology and small size of gold grains, i.e., high surface area to volume ratio increased by μm-scale surface dissolution textures, would have enhanced their propensity to float. The liberation of buoyant gold grains and secondary gold particles could contribute to rapid gold mobility and dispersion in natural environments.
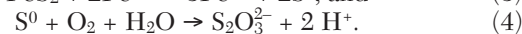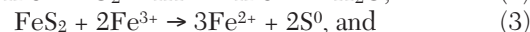
Introduction

The geochemical weathering of primary metal sulfide ores and the processes involved in supergene enrichment of precious metals, such as gold, have been well documented (Sillitoe and Lorson, 1994; Sillitoe and McKee, 1996). While these processes are mechanistically abiotic, the geochemistry of supergene ore deposits is influenced in part by bacterially catalyzed redox reactions within natural weathering environments (Nordstrom and Southam, 1997; Nordstrom and Alpers, 1999; Edwards et al., 2000b; Southam and Saunders, 2005; Enders et al., 2006; Rainbow et al., 2006; Zammit et al., 2015). From an economic perspective, metal mobility and enrichment at the Earth's surface have effectively focused exploration strategies in surficial weathering environments and have advanced the application of bioleaching of low-grade ore and "waste" tailings (Kelley et al., 2006; Rawlings and Johnson, 2007; Myagkaya et al., 2013; Schippers et al., 2014).

In the context of supergene gold enrichment processes, the mobility of gold has been attributed to thiosulfate and chloride ions—two ligands able to form soluble gold complexes, depending on the geochemistry of the environment (Boyle, 1979). However, these soluble gold complexes are destabilized in the presence of chemolithotrophic bacteria, i.e., iron- and sulfur-oxidizing bacteria and sulfate-reducing bacteria that act as a reducing agent, resulting in the formation elemental gold colloids (Lengke and Southam, 2006,

2007; Shuster et al., 2013, 2014). With respect to gold biogeochemistry, these chemolithotrophic bacteria have been shown to contribute to a continuum of gold dissolution and reprecipitation processes (Reith et al., 2007, 2013; Shuster and Southam, 2014).

In natural weathering, i.e., acid rock drainage (ARD), environments, acidophilic, iron- and sulfur-oxidizing bacteria catalyze the oxidation of metal sulfide minerals at a vastly higher rate than abiotic processes (Ehrlich, 1964; Singer and Stumm, 1970; Fowler and Crundwell, 1999; Hedrich et al., 2011). As a result, these chemolithotropic bacteria sustain low pH and increased ferric iron and thiosulfate concentrations that characterize the geochemical conditions of ARD environments (Nordstrom and Southam, 1997; Schippers and Sand, 1999; Shuster et al., 2014) through reactions 1 to 4:

$$FeS_2 + 6Fe^{3+} + 3H_2O \rightarrow S_2O_3^{2-} + 7Fe^{2+} + 6H^+, \quad (1)$$
$$4Fe^{2+} + O_2 + 4H^+ \rightarrow 4Fe^{3+} + 2H_2O, \quad (2)$$
$$FeS_2 + 2Fe^{3+} \rightarrow 3Fe^{2+} + 2S^0, \text{ and} \quad (3)$$
$$S^0 + O_2 + H_2O \rightarrow S_2O_3^{2-} + 2\,H^+. \quad (4)$$

The effect of biogeochemical weathering on primary gold-bearing, metal sulfide ore is important because it can lead to supergene gold enrichment and provides insight on the evolution of ore deposits over time. However, an unanswered question is the extent to which acidophilic, iron- and sulfur-oxidizing bacteria can influence the occurrence of gold during the initial stage of biogeochemical weathering. Here we demonstrate the link between the bacterially catalyzed dissolution of metal sulfides from a gold-bearing ore and the formation of secondary gold grains.

† Corresponding author: e-mail, j.shuster@uq.edu.au
*Current address: School of Earth Sciences, University of Queensland, Steele Building, Staff House Road, St. Lucia, QLD 4072, Australia

Methods

Mineralogical and structural characterization of gold-bearing ore

The Capillitas mine, located in the province of Catamarca, Argentina, is composed of a sequence of intermediate-sulfidation epithermal veins (Márquez-Zavalía et al., 1999; Márquez-Zavalía and Craig, 2004). A small, cm-scale sample of gold-bearing ore was obtained from the San Salvador vein ca. 180 m deep. The ore was cut into two billets, each ca. 20 × 20 × 3 mm. The billets were then polished to obtain "fresh" surfaces with comparable areas of ore and gangue minerals.

The polished billets were coated with 5-nm C deposition using a Hummer VI Sputter Coat Unit. Electron microprobe (EMP) analysis was performed on both billets using a JEOL JXA-8600 EMP operating at 15 kV with a defocused beam to determine the mineralogical assemblage and gold fineness. Repeated count times (20 s) were performed for elements and for mineral standards.

The polished billets were then analyzed using a LEO Ziess 1540XB field emission gun-scanning electron microscope (FEG-SEM), operating at an accelerating voltage of 1 or 10 kV and equipped with an Oxford Instruments INCAx-sight energy dispersive spectrometer (EDS) to image the mineral structures. The total number of gold grains was counted on each polished surface of the billets. The total surface areas of ore and gangue minerals were calculated by analyzing micrographs.

Iron- and sulfur-oxidizing bacterial enrichment and enumeration

An acidophilic, iron- and sulfur-oxidizing bacterial consortium was collected from Rio Tinto, Huelva, Spain (Preston et al., 2011; Shuster et al., 2014). Rio Tinto was chosen because metal resistant iron- and sulfur-oxidizing bacteria, i.e., *Leptospirillum ferrooxidans* and *Acidithiobacillus ferrooxidans,* constitute the microbial community from this site (Dopson et al., 2003; Gónzalez-Toril et al., 2003). Bacterial enrichments were made by inoculating 0.5-mL aliquots of the Rio Tinto consortium into sterile Fisherbrand® 13- × 100-mm borosilicate glass test tubes containing modified growth media defined by Silverman and Lundgren (1959). Growth medium contained 4 mL of basal salt solution (3 mM $(NH_4)_2SO_4$, 0.6 mM K_2HPO_4, 1.6 mM $MgSO_4 \cdot 7H_2O$) and 0.5 mL of 120 mM $FeSO_4 \cdot 7H_2O$, with pH adjusted to 2.3 using 2 M H_2SO_4. Test tubes were covered with sterile plastic push caps and were aerobically incubated at ca. 22°C for 3 weeks until the walls of tubes were coated in an iron hydroxysulfate mineral precipitate, i.e., a phenotypic indication of positive growth in the enrichments (Sasaki et al., 2006). Using the most probable number (MPN) statistical method (Cochran, 1950), the viable population of bacteria in the enrichment was 2.4×10^5 bacteria/mL. For this MPN, the bacterial enrichment was diluted in a 10-fold serial dilution using sterile test tubes and "fresh" growth media. This serial dilution were performed in quintuplet and incubated under the same conditions described above.

Construction of experimental system

An experimental system was constructed in a 125-mL-volume Erlenmeyer flask to represent a simplified ARD environment in which a gold-bearing ore could be exposed to biogeochemical weathering. The fluid phase of the system contained 90 mL of basal salt solution with adjusted pH as described for bacterial enrichments. A 10-mL inoculum of the enriched bacterial consortium (2.4×10^6 bacteria) plus any suspended μm-scale iron hydroxysulfate mineral precipitates (Preston et al., 2011; Shuster et al., 2014) were added to the experimental system. The flask was gently agitated for 1 min to evenly disperse the bacterial cells within the fluid phase. Based on the size of the billets and the inoculum, attachment of all bacteria to the mineral surface (Mielke et al., 2003) would produce ca. 0.1% coverage.

The billets that had been characterized using SEM were sonicated for 5 min, then rinsed three times with 75% ethanol followed by filter-sterilized (0.1-μm pore-size filter), deionized water to remove the C coating. The first billet was attached to a sterile polyethylene twine and vertically suspended in the fluid phase of the experimental system so that the polished surface was perpendicular to the bottom of the flask. This setup ensured that any cells found on the polished surface could be attributed to active processes, e.g., motility and attachment, and not to the accumulation of cells settling over time. The mouth of the flask was covered with sterile aluminum foil to prevent potential airborne contamination but allowed the system to be at equilibrium with the atmosphere. An abiotic control was constructed in a similar manner using the second billet; however, this control did not include a bacterial inoculum. The experimental system and abiotic control were incubated aerobically at ca. 22°C for 1 week and 2 months, i.e., exponential- and stationary-growth phases, respectively. Note that, due to limited ore sample, incubation periods were performed on the same billet to compare bacteria-mineral interactions at these growth phases. Large bacterial populations and a large water:rock ratio were used in this study so that biogeochemical effects could be analyzed under laboratory conditions within a practicable timeframe.

Soluble metal analysis from experimental system

Triplicate 5-mL aliquots were sampled from the experimental system and abiotic control at the initial construction and after 1-week and 2-month incubations. After aliquots were sampled, equivalent volume of filter-sterilized and pH-adjusted basal salt solution was added to the experimental system and abiotic control to maintain a consistent volume in the flasks so that soluble metal concentrations could be compared over time. The sampled aliquots were passed through a 0.1-μm pore-size filter to remove any solid material prior to measuring pH using a Denver Instrument Basic pH/Eh Meter with glass-body electrode calibrated to pH 2 and 4 (±0.03 pH units) reference standards. The filtered aliquots were then acidified to pH 1 using 70% ULTREX® II nitric acid and analyzed for soluble Ag, As, Au, Cu, Fe, Pb, Zn, and S using Perkin-Elmer Optima 3300-DV inductively coupled plasma-atomic emission spectroscopy (ICP-AES). High Purity™ standards were purchased from Delta Scientific and used for ICP-AES analysis.

Structural and chemical characterization of the weathered ore and gold grains

After 1 week, the suspended billets were removed from the experimental system and the abiotic control, fixed with 2%$_{(aq)}$

glutaraldehyde for 24 h, dehydrated in sequential 25, 50, 75, and 3 × 100%$_{(aq)}$ ethanol series, and dried using a Tousimis Research Corporation Samdri-PVT-3B critical point drier. The billets were coated with a 5-nm Os deposition using a Denton Vacuum Desk II coater sputter and characterized using the same FEG-SEM. After characterization, the billets were sonicated and rinsed as previously described to remove the coating, then resuspended into the respective flasks. After 2 months, the billets were removed from the flasks, prepared, and recharacterized in the same manner.

In the experimental system, solid material, i.e., μm- to sub-mm-scale fragments of the billet and secondary mineral precipitates, accumulated at the bottom of the flask during 2 months of incubation. By decanting the fluid phase, the solid material was concentrated into one-tenth of the total fluid volume, i.e., 10 mL, and was then transferred into a sterile Petri dish. Samples of solid material and eight gold grains were recovered from the bottom of the Petri dish and floating on the water's surface, respectively using a dissecting microscope, sterile forceps, and a metal probe. Solid material and gold grains were fixed with 2%$_{(aq)}$ glutaraldehyde, dehydrated, and dried using the same method described for the billets and placed on a 12-mm-diameter, aluminum stub with a carbon adhesive tab. The grains were coated with a 5-nm Ir deposition using a Bal-Tec sputter coater and analyzed using a JEOL JSM-7100F FEG-SEM equipped with a JEOL EDS analysis system operating at an accelerating voltage of 1 or 15 kV for surface imaging and quantitative chemical analysis, respectively.

After SEM analysis, one grain with gold nanoparticles occurring within surficial crevices was placed into a 1-mL-volume Eppendorf tube containing 30 μL of filter-sterilized, distilled deionized water. The Eppendorf was placed in a Soniclean® ultrasonic bath for 15 min to remove gold nanoparticles from the grain surface and suspend the nanoparticles in the fluid. Whole-mount transmission electron microscope (TEM) samples were prepared by placing 10-μL aliquots of this fluid onto three, separate Formvar-carbon coated 200-square mesh copper grids. Residual water was removed and the samples were analyzed using a JEOL 1010 TEM operating at 100 kV.

Results and Discussion

Mineral assemblage of the gold-bearing ore

The ore mineral assemblage of the billets was composed of sulfide, telluride, and tungstate minerals, based on EMP analysis. This assemblage included chalcopyrite ($CuFeS_2$), pyrite (FeS_2), galena (PbS), enargite (Cu_3AsS_4), hübnerite ($MnWO_4$), stannite (Cu_2FeSnS_4), arsenopyrite (FeAsS), goldfieldite ($Cu_{10}Te_4S_{13}$), and tetradymite (Bi_2Te_2S). This assemblage was consistent with previous studies by Márquez-Zavalía and Craig (2004). Sulfide minerals contained some μm-scale fissures and constituted ca. 11.3 and 10.7% of the total polished surface area of the first (experimental system) and second (abiotic control) billet.

Gold grains contained 89.92 ± 3.06% Au, 9.00 ± 1.9% Ag, and 1.07 ± 2.6% Cu, based on EMP analysis. This Au:Ag:Cu ratio of 10:1:0.1 is consistent with Márquez-Zavalía and Craig (2004). Gold grains were irregular in shape, less than 100 μm in size, and were hosted within a quartz matrix (Fig. 1). The
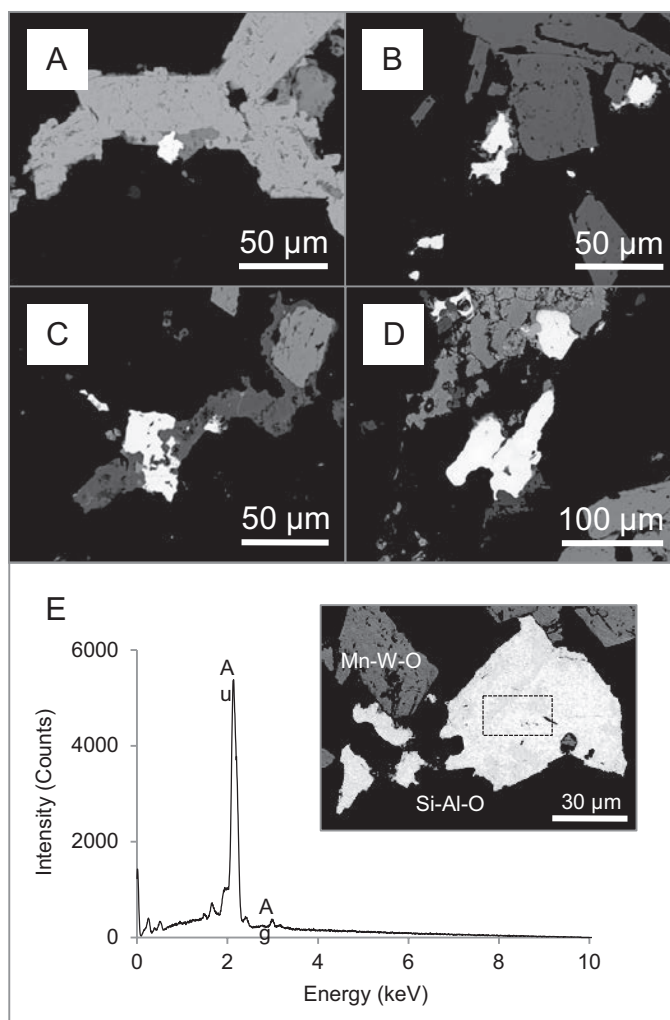

Fig. 1. Backscattered electron microprobe micrographs of four regions containing gold grains on the billets prior to experimental use (A-D). Gold grains contained Ag, based on backscattered SEM-EDS analysis (E), and grains were irregularly shaped (E, inset).

first and second billet contained a total of 17 and 23 visible gold grains, respectively.

Bacterial colonization of gold-bearing ore

Iron- and sulfur-oxidizing bacteria are known to preferentially attach onto metal sulfide mineral surfaces (Edwards et al., 2000a, b; Rodríguez et al., 2003; Africa et al., 2013). After 1 week, rod-shaped bacteria had colonized the polished surface of the billet (Fig. 2A). Both the experimental system and abiotic control remained at pH 2.3. After 2 months, a greater abundance of bacilli (rod-shaped) and spirillum bacteria were observed on the polished surface and demonstrated extracellular precipitation of nanometer-size minerals (Fig. 2B). The acidity of the experimental system decreased to pH 2.1 while the abiotic control remained at pH 2.3. The change in pH indicated that the bacterial consortium was metabolically active (Silverman and Lundgren, 1959). In the experimental system, bacterial attachment was demonstrated since the suspended ore represented the only source of Fe^{2+} or S^{2-} that could be used as the source of energy during metabolism of iron- and
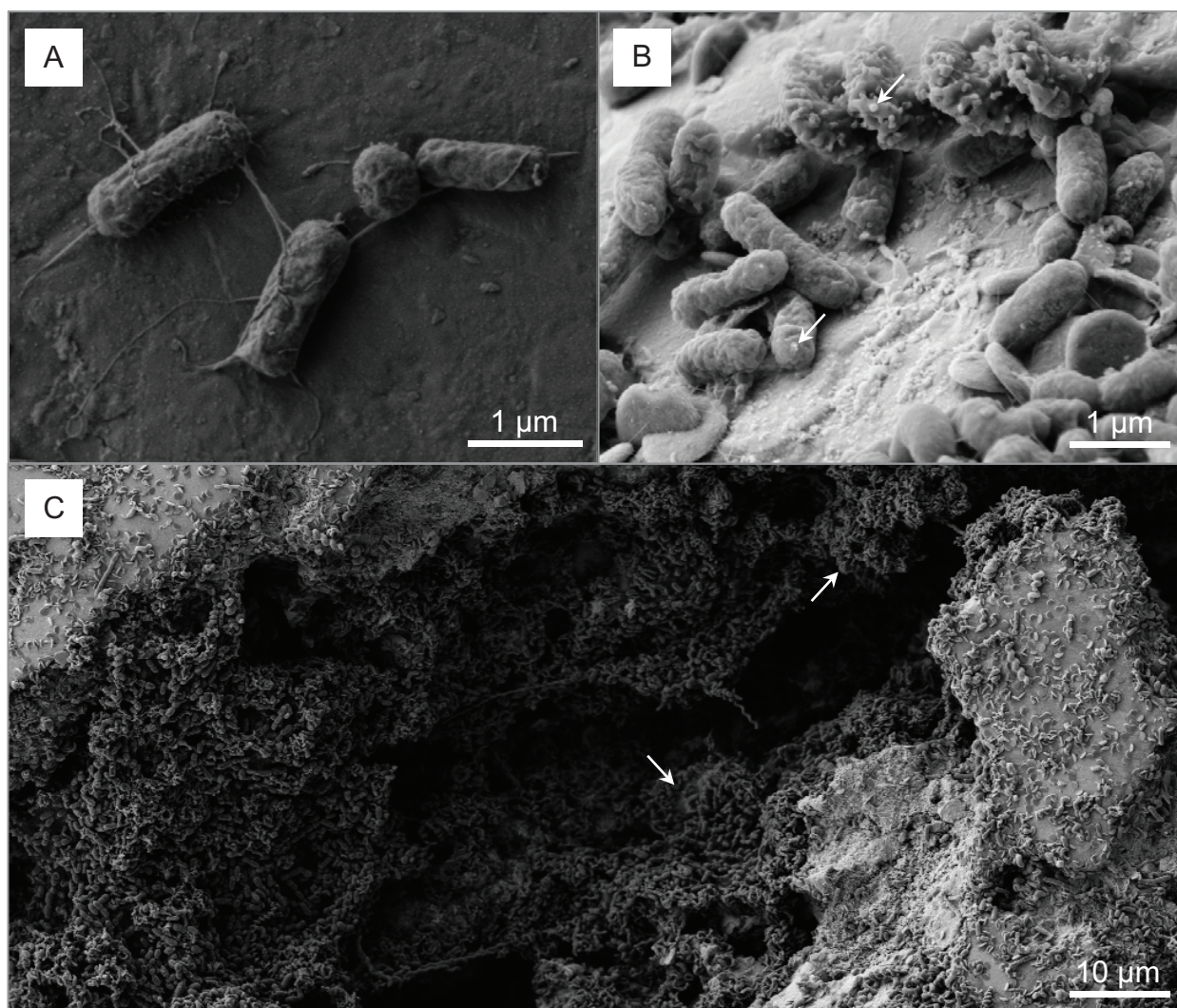
Fig. 2. High-resolution, secondary electron (SE) and backscattered SEM micrographs of bacteria occurring on the surface of the polished billet suspended in the experimental system over time. After 1 week, rod-shaped bacterial cells appear to be attached to the polished surface of the billet (A). After 2 months, a greater abundance of rod-shaped and spirillum bacteria appear to be attached to the polished surface (B) and exhibit nanometer-scale minerals on the extracellular surface (B, arrows). Extensive biofilms were also observed within crevices after 2 months (C, arrows). Bacterially catalyzed dissolution of iron- and sulfur-bearing minerals presumably created more crevices, which were ideal niches for further biofilm formation.

sulfur-oxidizing bacteria. Regions that once possessed metal sulfide minerals now appeared as μm- to sub-mm-scale dissolution pits with distinctive edges where grain boundaries once occurred. Furthermore, these pits contained abundant biofilms, indicating growth of the bacterial consortium (Fig. 2C). In natural ARD environments and this laboratory model, fissures and dissolution pits would provide additional surface area for biofilm formation (Walker and Pace, 2007).

Bacterial weathering of metal sulfides

After 2 months, Ag, As, Cu, Pb, and Zn were detected in the fluid phase of the experimental system and lower As, Cu, Pb, and Zn concentrations were detected within the abiotic control. Note that fractions of soluble Fe and S in the experimental system and S in the abiotic control were from the bacterial inoculum and basal salt solution, respectively (Table A1). Greater metal sulfide, i.e., $CuFeS_2$, FeS_2, and $FeAsS$, dissolution in the

experimental system was attributed to the bacterial consortium, whereas dissolution in the abiotic control was attributed to ferric iron and acid leaching by the fluid phase (Nesbitt et al., 1995). Bacterially catalyzed dissolution of metal sulfides also explains the extensive alteration of the polished surface (Fig. 3A, B) and the reduced structural integrity of the billet that resulted in the gangue and ore mineral fragments observed at the bottom of the experimental system (Fig. 3C).

In the experimental system, iron concentrations decreased after 2 months and were most likely an underestimate of the total amount of iron dissolved from the iron-bearing sulfide minerals. *Acidithiobacillus ferrooxidans* produce jarosite-group minerals as a by-product of active metabolism (Sasaki et al., 2006). Secondary mineral precipitates at the bottom of the experimental system were composed of Fe, O, S, P, and K, based on EDS analysis (Fig. 3D). These biogenic, secondary iron hydroxysulfate minerals, produced by bacterial weathering,
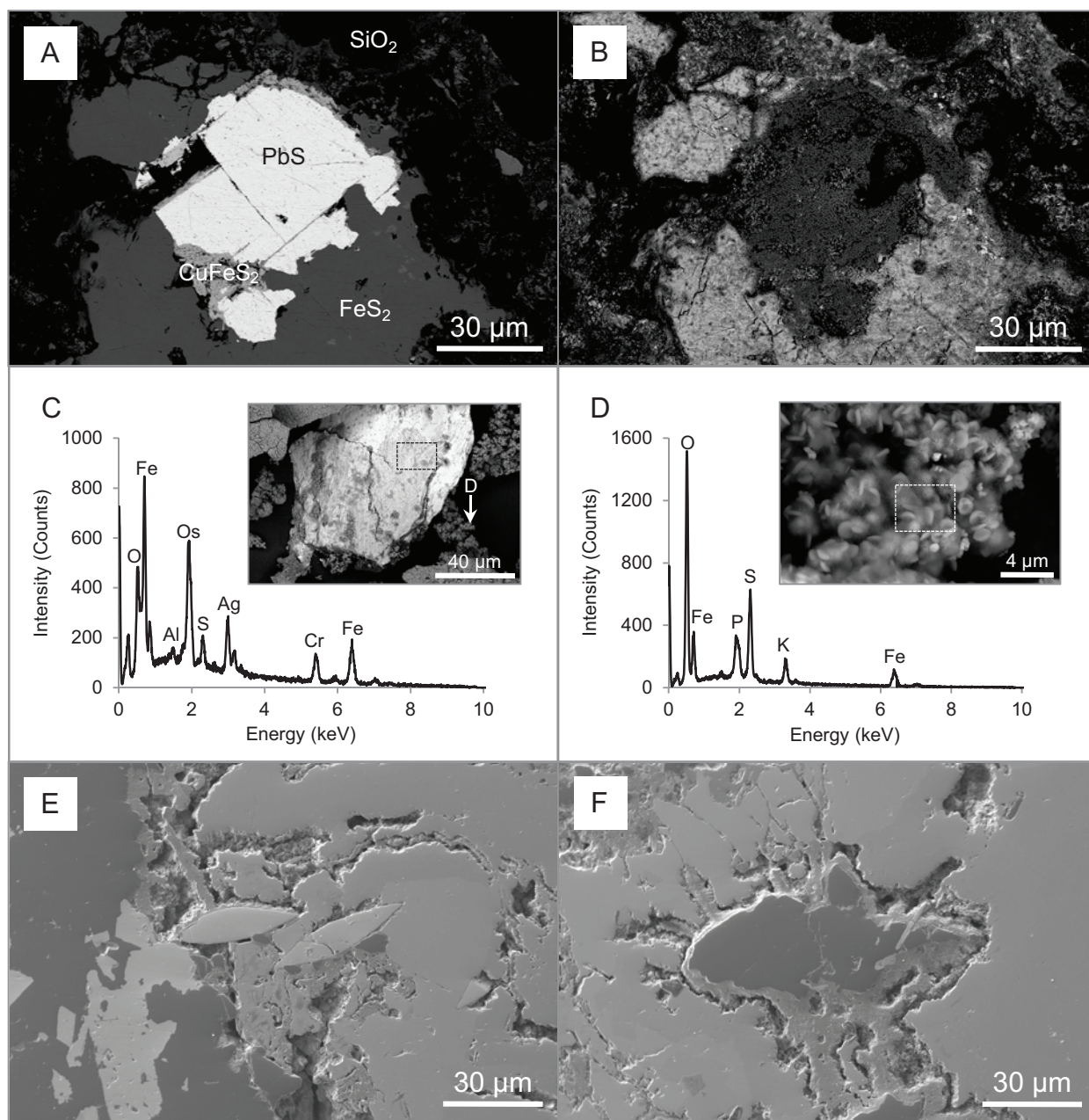
Fig. 3. A, B. Backscattered SEM micrograph of a region containing metal sulfide minerals on the polished surface of the billet prior to use in the experimental system (A). After 2 months of exposure, biofilms colonized the polished surface and altered the appearance of the original features (B). Note that adjusted brightness and contrast were required during analysis to reidentify mineral structures after the exposure to bacteria. C. Backscattered SEM micrograph of a fragment containing silver from the billet that sank to the bottom of the experimental system. D. Backscattered SEM micrograph of the secondary mineral precipitate that occurred at the bottom of the experimental system. This mineral precipitate was composed of Fe, O, K, S, and P, based on SEM-EDS analysis. E, F. SE-SEM micrograph of the billet prior to use in the abiotic control (E) and after 2 months (F); no changes to the surface textures were observed.

are responsible for the underestimated iron concentrations. No alterations to surface textures of the billet or secondary mineral precipitates were observed in the abiotic control (Fig. 3E, F).

Gold grain recovery

No gold grains were recovered from the abiotic control; however, eight gold grains were recovered from the experimental system. Seven of these grains were floating on the surface

of the fluid, and one grain with an iron hydroxide mineral coating (Fig. 4A, B) was recovered from the bottom of the Petri dish. It should be noted that decanting the fluid phase of the experimental system was performed as a conventional method for targeting gold grains that had presumably settled due to gravity. In hindsight, it is likely that some grains may have been lost during the decanting process, since most of the recovered gold grains were floating.
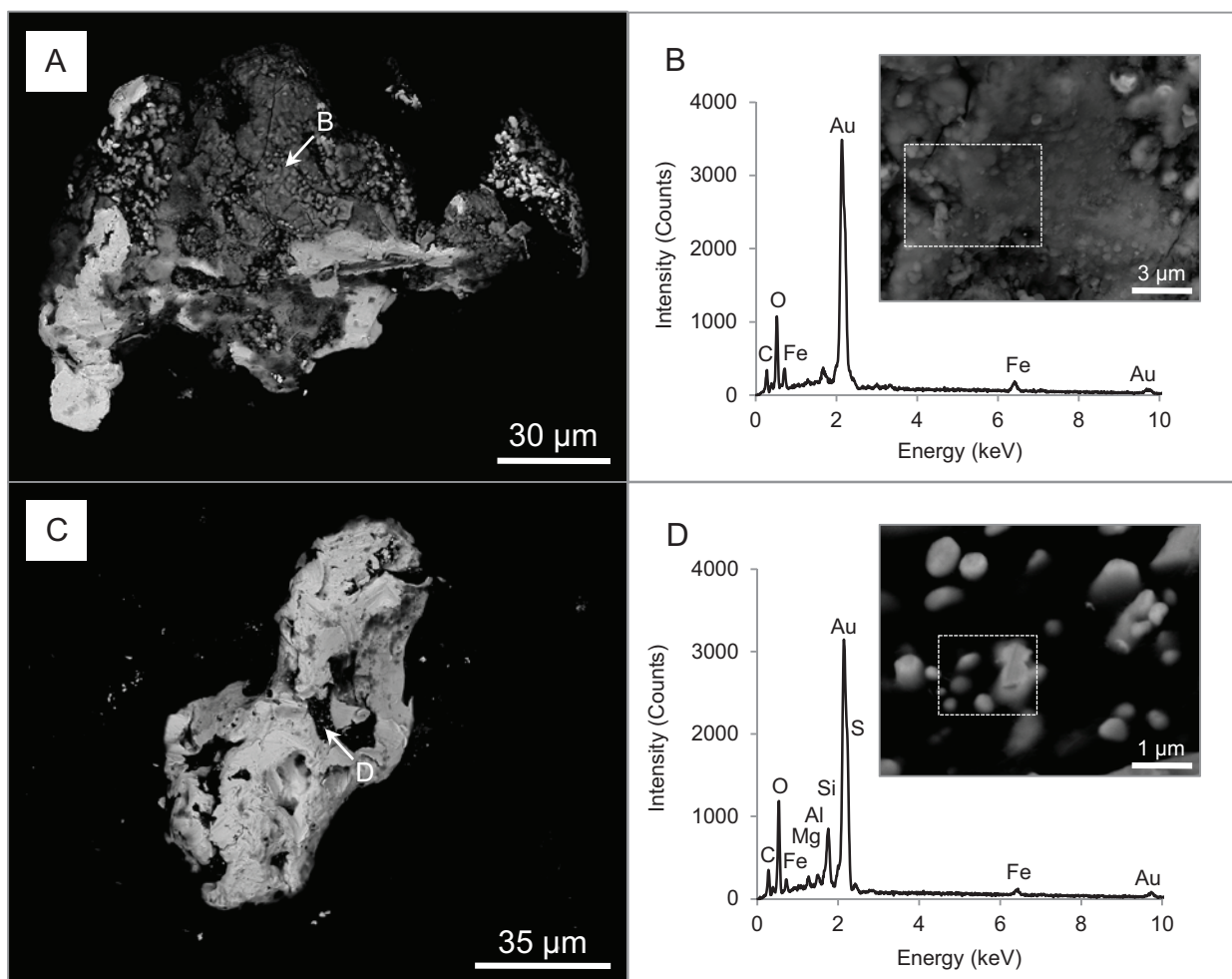
Fig. 4. A, B. Backscattered SEM micrograph of the gold grain that was recovered from the bottom of the Petri dish (A) that contained an iron hydroxysulfate coating (B). C. Backscattered SEM micrograph of a buoyant gold grain containing secondary gold nanoparticles that appeared embedded in detrital material within a crevice (arrow). D. Detrital material was composed of C, O, Al, Mg, Si, and Fe, based on SEM-EDS analysis.

Gold grains were less than 80 μm in size (maximum dimension: length and breadth) and were flake-like in shape with a range of creviced surface textures. These crevices contained detrital material composed of Si, O, Al, Mg, Fe, and S (Fig. 4C, D) and were likely derived from the dissolution of both aluminosilicate and iron-bearing sulfide minerals. Crevices also contained varying amounts of μm-size bacteriomorphic gold structures that were depleted in Ag, based on SEM-EDS analysis (Fig. 5A, B). These structures were analogous to others that have been documented on gold-enriched rims of placer electrum grains (Groen et al., 1990). More importantly, bacteriomorphic structures did not occur at gold grain boundaries on the polished surface of the billet prior to use in the experimental system. Bacterially catalyzed dissolution of metal sulfides results in the formation of thiosulfate and polythionate ligands (Schippers and Sand, 1999). With excess soluble S and Cu, the biogeochemical conditions of the experimental system could have promoted Cu-catalyzed thiosulfate leaching of silver from the gold grains, resulting in the detection of soluble Ag (Zipperian and Raghavan, 1988) and the gold-enriched bacteriomorphic structures:

$$2\ Ag^0 + 4\ S_2O_3^{2-} + \tfrac{1}{2}\ O_2 + 2\ H^+$$
$$\rightarrow 2\ Ag(S_2O_3)_2^{3-} + H_2O. \qquad (5)$$
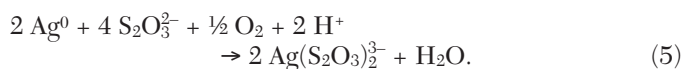
While the occurrence of soluble Au was below the ICP-AES detection limit, Cu-catalyzed thiosulphate leaching of gold could have also occurred (Zipperian and Raghavan, 1988; Abbruzzese et al., 1995; Groudev et al., 1996):

$$2\ Au^0 + 4\ S_2O_3^{2-} + \tfrac{1}{2}\ O_2 + 2\ H^+$$
$$\rightarrow 2\ Au(S_2O_3)_2^{3-} + H_2O \qquad (6)$$
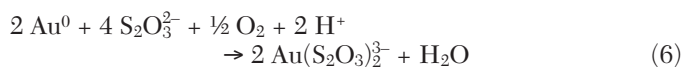
However, dissolved gold had reprecipitated as nanophase gold particles in the detrital material—i.e., possessing bacteria or bacterial exopolymer as a potential reducing agent (Fig. 5C). Nanophase gold occurred as octahedral platelets and colloids (Fig. 5D, E). These secondary gold structures demonstrate that gold dissolution and reprecipitation were occurring at the grain surface (Reith et al., 2010) concurrently with the weathering of the gold-bearing ore. The cooccurrence of euhedral crystals and colloids could be attributed to variations in pH, Au concentrations, and availability of gold-reducing agents (Grzelczak et al., 2008) within the microenvironments of crevices.
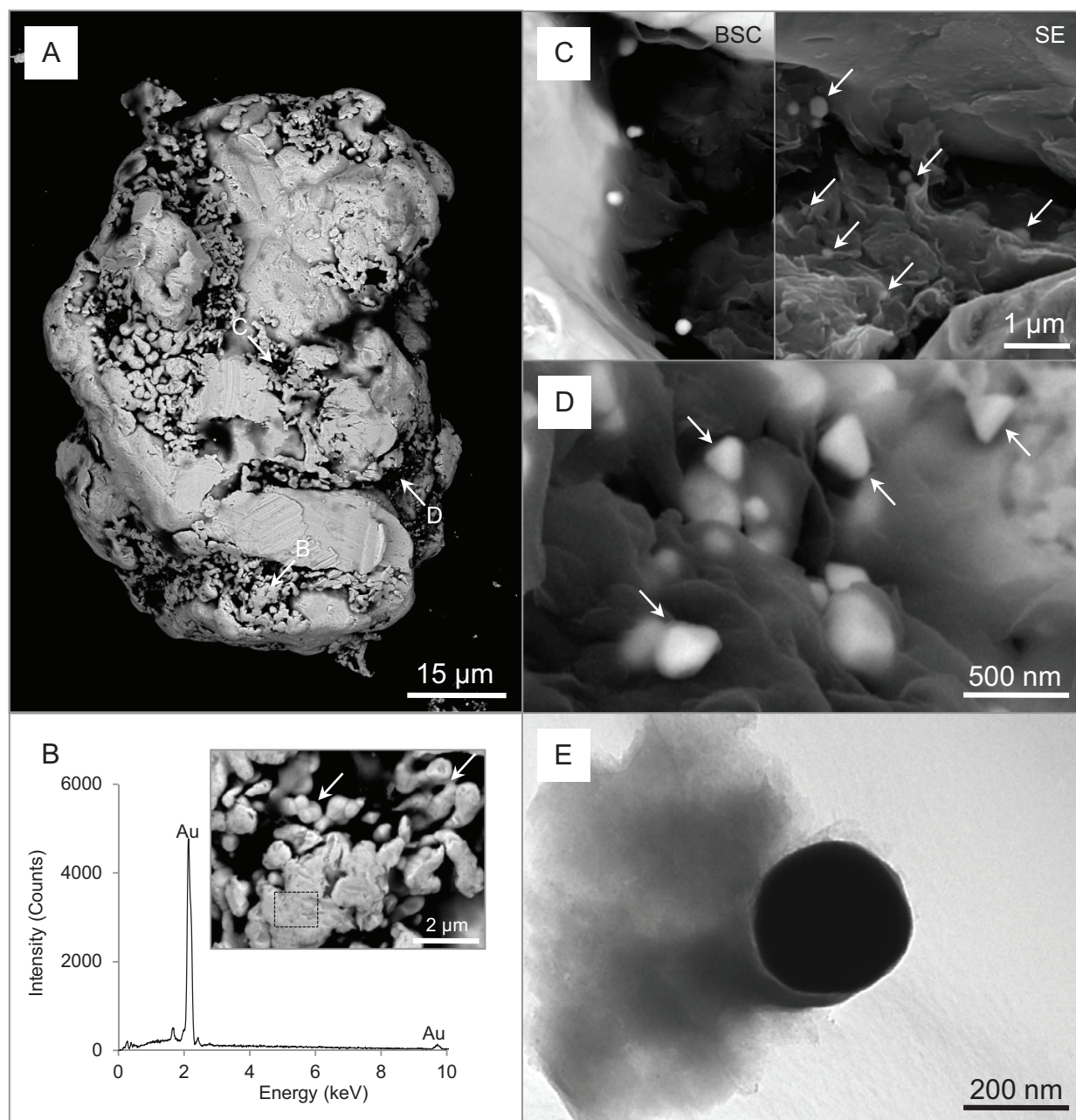
Fig. 5. Floating gold grains demonstrated varying degrees of weathered textures, i.e., rounded morphology and surficial crevices (A). Backscattered SEM analysis revealed that crevices contained bacteriomorphic structures that were enriched in gold (B). Backscattered SEM analysis demonstrated that nanophase gold particles occurred within crevices (C); however, SE-SEM of the same regions revealed that these particles were embedded within the detrital material (arrows). High-resolution backscattered SEM analysis revealed that nanophase gold particles were composed of octahedral platelets with varying crystallographic morphologies (D, arrows). Gold particles also occurred as colloids that were less than 300 nm in diameter, based on TEM analysis (E). BSC = backscattered, SE = secondary electron.

Buoyancy of gold grains and the difficulty of recovering fine gold particles from placer deposits are attributed to various factors, including hydrophobicity of the mostly "fresh" gold surface, organic material, flake-like morphologies of grains, and porosity such as crevices (Wenqian and Poling, 1983). It is possible that thiosulfate leaching of silver could have increased gold fineness of the grains along with porosity at the grain surface, i.e., bacteriomorphic structures, and therefore contributed to the buoyancy of grains. In contrast, the hydrated iron hydroxysulfate coating would have made the grain surface hydrophilic, causing this specific grain to sink. In natural environments, hydrophobicity would promote the transport of gold grains by allowing them to float above sediments within streams, which could contribute to the dispersion of gold (Freyssinet et al., 1989).

Conclusion

Bacteria can have an influence on the mobility of gold within weathering environments. In this study, the experimental system demonstrated the extent in which an enriched bacterial consortium of acidophilic, iron- and sulfur-oxidizing bacteria could attach to a gold-bearing ore as a substrate. Increased acidity and the development of an extensive biofilm with extracellular precipitation of nm- to μm-sized mineral precipitates on the suspended billet indicated growth and active metabolism of the bacterial consortium. Bacterial-catalyzed dissolution of metal sulfide minerals was supported by the detection of soluble Ag, As, Cu, Pb, and Zn in the fluid phase of the experimental system. The detection of soluble Ag and the presence of gold-rich bacteriomorphic structures on floating grain surfaces suggest that Cu-catalyzed thiosulfate leaching could have occurred. This laboratory model provides a link between the biogeochemical weathering of a gold-bearing ore and the initial formation of gold grains containing bacteriomorphic structures, colloids, and octahedral platelets. Furthermore, the buoyancy of gold grains highlights a potential mechanism in which gold could be distally transported within surficial environments. Although the rate of biooxidation was accelerated in vitro, these same processes would correspondingly occur in a natural weathering environment, resulting in gold dispersion over seasonal to decadal time scales.

Acknowledgments

REFERENCES

Abbruzzese, C., Fornari, P., Massidda, R., Vegliò, F., and Ubaldini, S., 1995, Thiosulphate leaching for gold hydrometallurgy: Hydrometallurgy, v. 39, p. 265–276.

Africa, C.J., van Hille, R.P., and Harrison, S.T., 2013, Attachment of *Acidithiobacillus ferrooxidans* and *Leptospirillum ferriphilum* cultured under varying conditions to pyrite, chalcopyrite, low-grade ore and quartz in a packed column reactor: Applied Microbiology and Biotechnology, v. 97, p. 1317–1324.

Boyle, R.W., 1979, The geochemistry of gold and its deposits: Geological Survey of Canada Bulletin, v. 280, p. 1–54.

Cochran, W.G., 1950, Estimation of bacterial densities by means of the "most probable number": Biometrics, v. 6, p. 105–116.

Dopson, M., Baker-Austin, C., Koppineedi, P.R., and Bond, P.L., 2003, Growth in sulfidic mineral environments: Metal resistance mechanisms in acidophilic micro-organisms: Microbiology, v. 149, p. 1959–1970.

Edwards, K., Bond, P., and Banfield, J., 2000a, Characteristics of attachment and growth of *Thiobacillus caldus* on sulphide minerals: A chemotactic response to sulphur minerals: Environmental Microbiology, v. 2, p. 324–332.

Edwards, K.J., Bond, P.L., Druschel, G.K., McGuire, M.M., Hamers, R.J., and Banfield, J.F., 2000b, Geochemical and biological aspects of sulfide mineral dissolution: Lessons from Iron Mountain, California: Chemical Geology, v. 169, p. 383–397.

Ehrlich, H.L., 1964, Bacterial oxidation of arsenopyrite and enargite: Economic Geology, v. 59, p. 1306–1312.

Enders, M.S., Knickerbocker, C., Titley, S.R., and Southam, G., 2006, The role of bacteria in the supergene environment of the Morenci porphyry copper deposit, Greenlee County, Arizona: Economic Geology, v. 101, p. 59–70.

Fowler, T.A., and Crundwell, F.K., 1999, Leaching of zinc sulfide by *Thiobacillus ferrooxidans*: Bacterial oxidation of the sulfur product layer increases the rate of zinc sulfide dissolution at high concentrations of ferrous ions: Applied and Environmental Microbiology, v. 65, p. 5285–5292.

Freyssinet, P., Lecomte, P., and Edimo, A., 1989, Dispersion of gold and base metals in the Mborguéné lateritic profile, east Cameroun: Journal of Geochemical Exploration, v. 32, p. 99–116.

Gónzalez-Toril, E., Gómez, F., Rodríguez, N., Fernández-Remolar, D., Zuluaga, J., Marín, I., and Amils, R., 2003, Geomicrobiology of the Tinto River, a model of interest for biohydrometallurgy: Hydrometallurgy, v. 71, p. 301–309.

Groen, J.C., Criag, J.R., and Rimstidt, J.D., 1990, Gold-rich rim formation on electrum grains in placers: Canadian Mineralogist, v. 28, p. 207–228.

Groudev, S.N., Spasova, I.I., and Ivanov, I.M., 1996, Two-stage microbial leaching of a refractory gold-bearing pyrite ore: Minerals Engineering, v. 9, p. 707–713.

Grzelczak, M., Perez-Juste, J., Mulvaney, P., and Liz-Marzan, L.M., 2008, Shape control in gold nanoparticle synthesis: Chemical Society Reviews, v. 37, p. 1783–1791.

Hedrich, S., Schlomann, M., and Johnson, D.B., 2011, The iron-oxidizing proteobacteria: Microbiology, v. 157, p. 1551–1564.

Kelley, D.L., Kelley, K.D., Coker, W.B., Caughlin, B., and Doherty, M.E., 2006, Beyond the obvious limits of ore deposits: The use of mineralogical, geochemical, and biological features for the remote detection of mineralization: Economic Geology, v. 101, p. 729–752.

Lengke, M., and Southam, G., 2006, Bioaccumulation of gold by sulfate-reducing bacteria cultured in the presence of gold(I)-thiosulfate complex: Geochimica et Cosmochimica Acta, v. 70, p. 3646–3661.

——2007, The deposition of elemental gold from gold (I) thiosulfate complexes mediated by sulfate-reducing bacterial conditions: Economic Geology, v. 102, p. 109–126.

Márquez-Zavalía, M.F., and Craig, J.R., 2004, Tellurium and precious-metal ore minerals at Mina Capillitas, northwestern Argentina: Neues Jahrbuch für Mineralogie Abhandlungen, v. 4, p. 176–192.

Márquez-Zavalía, M.F., Craig, J.R., and Solberg, T.N., 1999, Duranusite, product of realgar alteration, Mina Capillitas, Argentina: Canadian Mineralogist, v. 37, p. 1255–1259.

Mielke, R.E., Pace, D.L., Porter, T., and Southam, G., 2003, A critical stage in the formation of acid mine drainage: Colonization of pyrite by *Acidithiobacillus ferrooxidans* under pH-neutral conditions: Geobiology, v. 1, p. 81–90.

Myagkaya, I.N., Lazareva, E.V., Gustaitis, M.A., Zayakina, S.B., Polyakova, E.V., and Zhmodik, S.M., 2013, Gold in the sulfide waste-peat bog system as a behavior model in geological processes: Doklady Earth Sciences, v. 453, p. 1132–1136.

Nesbitt, H.W., Muir, I.J., and Pratt, A.R., 1995, Oxidation of arsenopyrite by air and air-saturated, distilled water, and implications for mechanism of oxidation: Geochimica et Cosmochimica Acta, v. 59, p. 1773–1786.

Nordstrom, D.K., and Alpers, C., 1999, Negative pH, efflorescent mineralogy, and consequences for environmental restoration at the Iron Mountain Superfund site, California: Proceedings of the National Academy of Sciences, v. 96, p. 3455–3462.

Nordstrom, D.K., and Southam, G., 1997, Geomicrobiology of sulphide mineral oxidation: Reviews in Mineralogy, Mineralogical Society of America, v. 35, p. 362–390.

Preston, L.J., Shuster, J., Fernandez-Remolar, D., Banerjee, N.R., Osinski, G.R., and Southam, G., 2011, The preservation and degradation of filamentous bacteria and biomolecules within iron oxide deposits at Rio Tinto, Spain: Geobiology, v. 9, p. 233–249.

Rainbow, A., Kyser, T.K., and Clark, A.H., 2006, Isotopic evidence for microbial activity during supergene oxidation of a high-sulfidation epithermal Au-Ag deposit: Geology, v. 34, p. 269–272.

Rawlings, D.E., and Johnson, D.B., 2007, The microbiology of biomining: Development and optimization of mineral-oxidizing microbial consortia: Microbiology, v. 153, p. 315–324.

Reith, F., Lengke, M.F., Falconer, D., Craw, D., and Southam, G., 2007, The geomicrobiology of gold: International Society for Microbial Ecology Journal, v. 1, p. 567–584.

Reith, F., Fairbrother, L., Nolze, G., Wilhelmi, O., Clode, P.L., Gregg, A., Parsons, J.E., Wakelin, S.A., Pring, A., Hough, R., Southam, G., and Brugger, J., 2010, Nanoparticle factories: Biofilms hold the key to gold dispersion and nugget formation: Geology, v. 38, p. 843–846.

Reith, F., Brugger, J., Zammit, C., Nies, D., and Southam, G., 2013, Geobiological cycling of gold: From fundamental process understanding to exploration solutions: Minerals, v. 3, p. 367–394.

Rodríguez, Y., Ballester, A., Blázquez, M.L., González, F., and Muñoz, J.A., 2003, Study of bacterial attachment during the bioleaching of pyrite, chalcopyrite, and sphalerite: Geomicrobiology Journal, v. 20, p. 131–141.

Sasaki, K., Sakimoto, T., Endo, M., and Konno, H., 2006, FE-SEM study of microbially formed jarosite by *Acidithiobacillus ferrooxidans*: Materials Transactions, v. 47, p. 1155–1162.

Schippers, A., and Sand, W., 1999, Bacterial leaching of metal sulfides proceeds by two indirect mechanisms via thiosulfate or via polysulfides and sulfur: Applied and Environmental Microbiology, v. 65, p. 319–321.

Schippers, A., Hedrich, S., Vasters, J., Drobe, M., Sand, W., and Willscher, S., 2014, Biomining: Metal recovery from ores with microorganisms: Advances in Biochemical Engineering/Biotechnology, v. 141, p. 1–47.

Shuster, J., and Southam, G., 2014, The in-vitro "growth" of gold grains: Geology, v. 43, p. 79–82.

Shuster, J., Marsden, S., Maclean, L.C.W., Ball, J., Bolin, T., and Southam, G., 2013, The immobilization of gold from gold (III) chloride by a halophilic sulphate-reducing bacterial consortium: Geological Society, London, Special Publications, v. 393, p. 249–263.

Shuster, J., Bolin, T., MacLean, L.C.W., and Southam, G., 2014, The effect of iron-oxidising bacteria on the stability of gold (I) thiosulphate complex: Chemical Geology, v. 376, p. 52–60.

Sillitoe, R.H., and Lorson, R., 1994, Epithermal gold-silver-mercury deposits at Paradise Peak, Nevada: Ore controls, porphyry gold association, detachment faulting and supergene oxidation: Economic Geology, v. 89, p. 1228–1248.

Sillitoe, R.H., and McKee, E.H., 1996, Age of supergene oxidation and enrichment in the Chilean porphyry copper province: Economic Geology, v. 91, p. 164–179.

Silverman, M.P., and Lundgren, D.G., 1959, Studies on the chemoautotrophic iron bacterium *Ferrobacillus ferrooxidans*: Journal of Bacteriology, v. 77, p. 642–647.

Singer, P.C., and Stumm, W., 1970, Acidic mine drainage: The rate-determining step: Science, v. 167, p. 1121–1123.

Southam, G., and Saunders, J.A., 2005, The geomicrobiology of ore deposits: Economic Geology, v. 100, p. 1067–1084.

Walker, J.J., and Pace, N.R., 2007, Endolithic microbial ecosystems: Annual Review of Microbiology, v. 61, p. 331–347.

Wenqian, W., and Poling, G.W., 1983, Methods for recovering fine placer gold: CIM Bulletin, v. 76, p. 47–56.

Zammit, C.M., Shuster, J.P., Gagen, E.J., and Southam, G., 2015, The geomicrobiology of supergene metal deposits: Elements, v. 11, p. 337–342.

Zipperian, D., and Raghavan, S., 1988, Gold and silver extraction by ammoniacal thiosulfate leaching from a rhyolite ore: Hydrometallurgy, v. 19, p. 361–375.

Table A1. Average Concentrations (µM) of Soluble Elements in the Experimental System and Abiotic Control

Element	Detection limit	Experimental system T_1	Experimental system T_2	Abiotic control T_1	Abiotic control T_2
Ag	0.09	--	0.46 ± 0.0	--	--
As	0.40	--	60.2 ± 0.48	--	0.53 ± 0.0
Au	0.25	--	--	--	--
Cu	0.16	--	712.9 ± 4.16	--	114.5 ± 1.28
Fe	0.90	$7,049 \pm 54.7$	$6,303 \pm 64.6$	--	16.53 ± 0.21
Pb	0.10	--	7.69 ± 0.06	--	0.26 ± 0.06
S	0.62	$6,871 \pm 36.0$	$10,977 \pm 108.0$	219.44^1	268.2 ± 32.5
Zn	0.15	--	28.1 ± 0.40	--	12.5 ± 0.15

Notes: Concentrations determined by ICP-AES analysis at the initial construction (T_1) and after 2 months of exposure (T_2); Fe and S concentrations in experimental system T_1 correspond to the bacterial inoculum, and the S concentration in the abiotic control T_1 corresponds to the basal salt solution
-- = below detection limit
[1] single measurement